Article

Inherently Chiral Bambus[4]urils

Amar Ramchandra Mohite, and Ofer Reany

J. Org. Chem., **Just Accepted Manuscript** • DOI: 10.1021/acs.joc.0c01174 • Publication Date (Web): 10 Jun 2020

Inherently Chiral Bambus[4]urils

Amar Ramchandra Mohite† and Ofer Reany†,*

† Department of Natural Sciences, The Open University of Israel, Ra'anana 4353701, Israel.
E-mail: oferre@openu.ac.il

Abstract

A new class of bambus[4]urils (BU[4]s) composed of asymmetric *N,N'*-disubstituted glycoluril subunits with different alkyl groups were designed, synthesized and fully characterized by NMR techniques and X-ray crystallography. Structural studies showed that four macrocyclic diastereoisomers are possible: two S_n symmetric achiral macrocycles and two macrocycles that are "inherently" chiral. The relative "head-to-tail" arrangement of the *N*-substituents in $Bn_4Me_4BU[4]$, **5a**, clearly observed by X-ray spectroscopy analysis, determine the overall symmetry of the bambusuril structure. Chiral $Pr_4Me_4BU[4]$, **4b**, was resolved by chiral HPLC into its enantiomers and all four inherently chiral bambusuril pairs (two $Pr_4Me_4BU[4]$ and two $Bn_4Me_4BU[4]$ stereoisomers, **4b**, **4d, 5b** and **5d**) were clearly observed by ^1H NMR spectroscopy with the aid of (*R*)-BINOL as a chiral solvating agent. This latter methodology provides a rapid and powerful approach for investigating the enantiopurity of inherently chiral cavitands, which complements and augments the conventional chromatographic approaches.

TOC

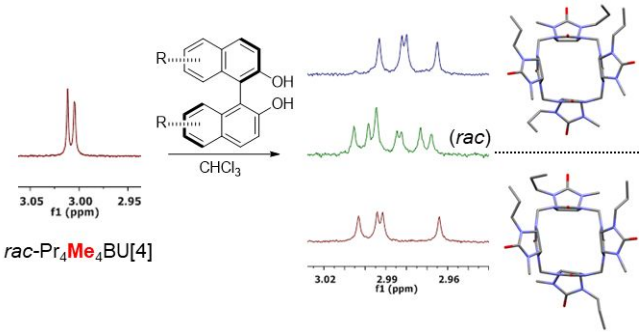

Introduction

Chirality in macrocycles with large cavities has attracted great attention due to their extensive use in chiral recognition, especially in their role for resolution of racemates and in selectively transporting chiral guests through bulk liquid membrane technologies.[1] In addition, chiral host systems are often regarded as enzyme mimics, acting as catalysts in asymmetric reactions to afford high yields and enantiomeric excess (*ee*) of chiral products.[2] Therefore, development of novel chiral receptors or supramolecular frameworks, provide tools for the stereochemical understanding of complex biological systems. For example, chiral cyclodextrins (CDs) have been used as artificial hosts mimicking various enzyme activities,[3] and chiral corands were utilized as transacylase mimics.[4] Similarly, chiral porphyrins have been designed to model oxygen uptake and oxygen transport processes,[5] and chiral crown-ethers were employed to mimic natural ion channels.[6]

Glycoluril-based cavitands such as cucurbiturils (CBs) and bambusurils (BUs) are rigid achiral macrocycles, exhibiting D_{nh} and S_n point group of symmetry, respectively. A general criterion for chirality is the absence of any improper symmetry elements, *i.e.* S_n, including mirror image,σ,

or a center of inversion, *i*. As such, these cavitands can be made chiral by either appending an intrinsically chiral functionality to the macrocyclic backbone or by using a non-symmetric subunit to produce stereogenic cavitands (Scheme 1). To date, several chiral macrocycles have been reported, including chiral hemicucurbiturils,[7] biotinurils[8] and chiral BU[6],[9] all of which are constructed from symmetrical cavity with stereogenic centers at their backbone or include tethered linkers with "external" stereogenic groups.

Chirality based on non-symmetric functionalization encompasses many examples of chiral calixarenes and resorcinarenes.[10] Hence, substituents strategically positioned may give rise to a macrocycle whose mirror image is not superimposable onto itself. In calixarenes, the expression inherently chiral was first coined by Bohmer *et al.*[11] and later extended by Mandolini, Schiaffino and co-workers[12] to include non-symmetrically substituted molecules that exhibit a curvature structure. In the last decade the concept of inherent chirality was demonstrated in the synthesis and applications of molecules that present curvature.[13,14] Interestingly, only rare examples of inherently chiral cucurbiturils are known in the literature[15] and, to the best of our knowledge, there are no reports of such chirality in bambusurils. (±)-bis-*nor*-*seco*-CB[6], was the first reported cavitand where enantio- and diastereoselective recognition was demonstrated by cavity selection, without the need for a chiral auxiliary.[16] Similarly, the *nor*-*seco*-CB[10][17] and the Eu^{+3} complex of twisted CB[14][18] exhibit asymmetric cavities but no applications in chiral recognition were demonstrated.

Recently, we introduced a new family of cavitands, dubbed *hetero*-bambus[n]urils (BU[n]s).[19] These macrocycles are rigid molecules due to the high steric demands of their subunits, which are locked in an alternate arrangement. Moreover, we demonstrated that sulfur analogs of BU[4], which are too small to accommodate any type of guest, have shown much potential for the formation of metal-organic chain polymers[20,21] and in anchoring self-assembled monolayers (SAMs) on gold surfaces.[22] Therefore, designing inherently chiral hetero-BUs would be appealing for developing applications in the field of chiral sensing technologies.

Here, we demonstrate a synthetic strategy for the preparation of a new family of bambus[4]urils (BU[4]s) composed of asymmetric *N,N'*-disubstituted glycoluril subunits with different alkyl groups (Scheme 1). Accordingly, the synthesis of $Pr_4Me_4BU[4]$ and $Bn_4Me_4BU[4]$ afforded mixtures of four possible diastereoisomers: two of which are symmetric achiral (S_4 and S_2 symmetry), and two "inherently" chiral macrocycles (C_1 and C_2 symmetry). Each one of the diastereoisomers was isolated and fully characterized by spectroscopic techniques including NMR and X-ray spectroscopy. The solid state structures of the achiral stereoisomers of $Pr_4Me_4BU[4]$ and $Bn_4Me_4BU[4]$ reveal two possible orientation modes, head-to-tail and head-to-head, derived from the different spatial orientation of the substituents around the bambusuril cavity. We also succeeded to separate between the enantiomers of each of the two inherently chiral bambusurils and determined their purity by ^1H NMR spectroscopy, using 1,1'-bi-2-naphthol (BINOL) derivatives as chiral solvating agents. We also show that the enantiomeric purity results obtained by this technique are closely matched to values determined by chiral HPLC analysis.

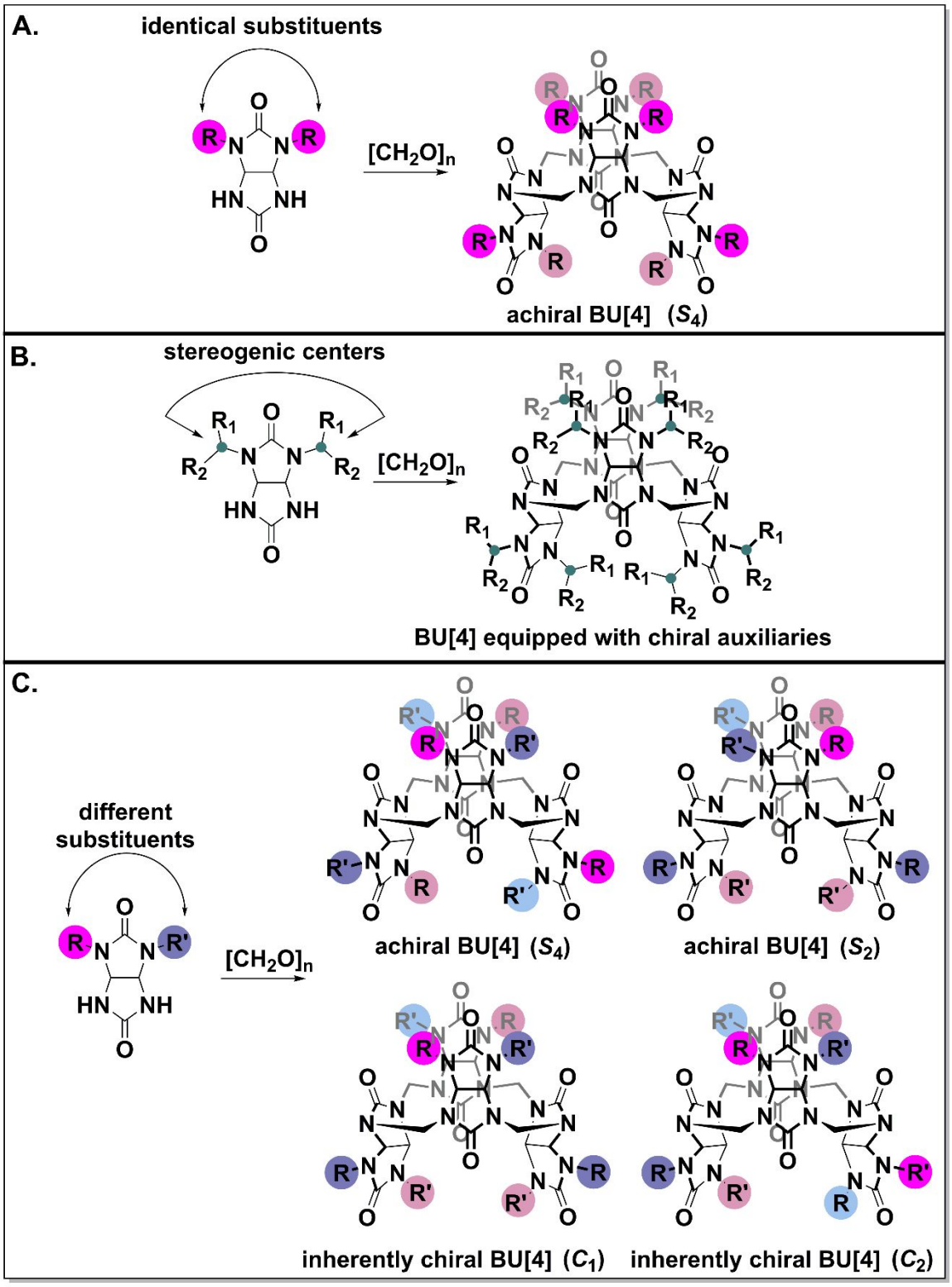

Scheme 1. Different categories of stereogenicity in BU[4]s depending on the alkyl group identity in *N*,*N*'-disubstituted glycoluril subunit: **A**. achiral BU[4], **B**. BU[4] equipped with stereogenic centers and **C**. BU[4] exhibiting four possible diastereoisomers: two of which are symmetric achiral (S_4 and S_2 symmetry), and two "inherently" chiral macrocycles (C_1 and C_2 symmetry).

Results and Discussion

Synthesis and characterization

For the synthesis of BU[4] with different *N*-substituents, asymmetric *N,N'*-disubstituted glycoluril bearing different alkyl substituents were initially prepared. Commercially available propyl or benzyl isocyanates were treated with methylamine to produce the corresponding asymmetric dialkyl ureas, followed by reaction with *trans*-4,5-dihydroxyimidazolidin-2-one (DHI)[23] to afford a mixture of enantiomeric glycoluril products, **3a** and **3b** (Scheme 2).

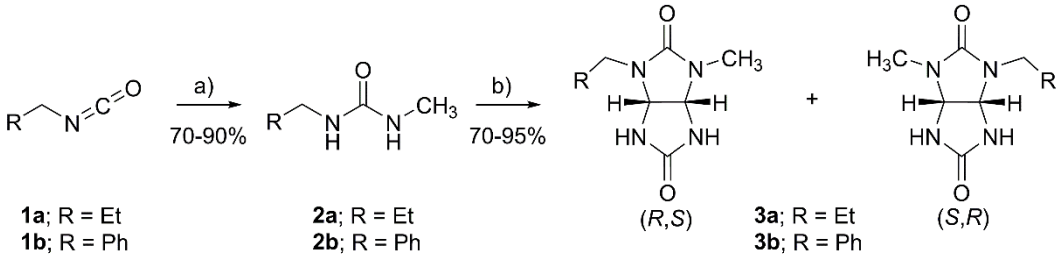

Scheme 2. Synthesis of asymmetric glycoluril (racemic mixture) from asymmetric dialkylurea. Conditions: a) $MeNH_2$ (1.5 equiv.), 0 °C for 2 h, then, *RT*, 6 h in dry THF; b) DHI (1.1 equiv.), con. HCl (0.1 mL), reflux in water, 1 h.

Condensation of the racemic mixtures of **3a** and **3b** with paraformaldehyde in acidic (PTSA) chloroform solution followed by microwave irradiation for 2 h, respectively afforded all possible $Pr_4Me_4BU[4]$ stereoisomers, **4a-d**, and $Bn_4Me_4BU[4]$ stereoisomers, **5a-d** in good overall yields(Figure 1). All stereoisomers could be separated by preparative TLC and fully characterized by NMR and HRMS (*vide infra* and in experimental section). Interestingly, significant amounts of every diastereomer could be found in the mixture and the ratio between the four stereoisomers was found to be 1:1:1:1 and 0.8:1:1:0.6, for **4** and **5** respectively.

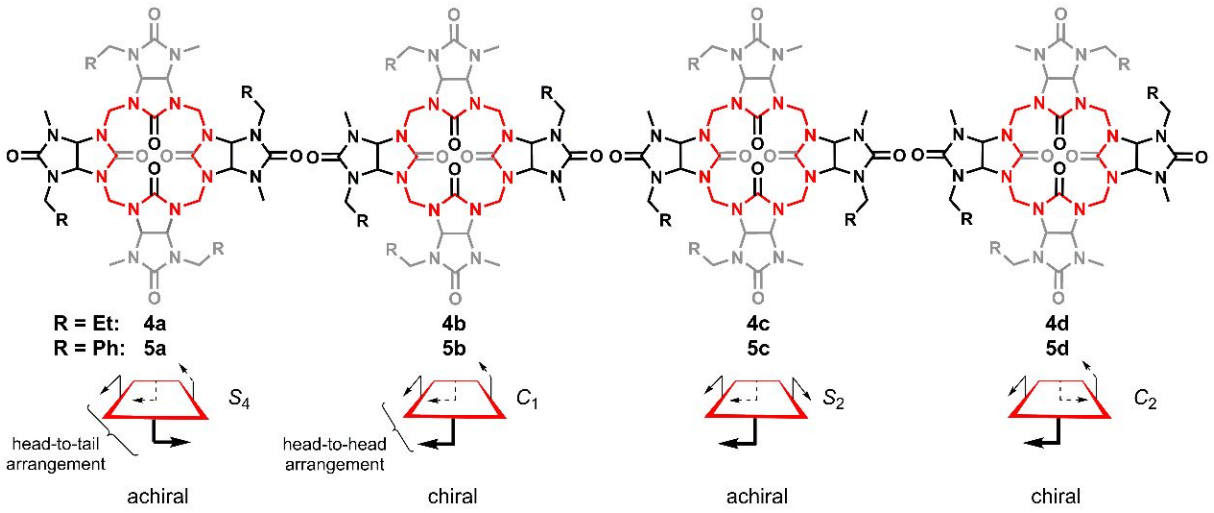

Figure 1. *Top:* drawings of all BU[4] diastereoisomers, **4a-d** and **5a-d** in 1,3-alternate structure (color code: red, a square plane representing the equator part of the bambusuril; black, dialkyl imidazolidinone rings above the square plane; grey, dialkyl imidazolidinone rings below the square plane). *Bottom*: schematic presentation of the larger substituents in all possible orientations. Arrowheads represent the larger group above or below the square plane of BU[4] in either head-to-tail or head-to-head arrangement.

The 1,3-alternate structure of BU[4] equipped with eight identical alkyl groups exhibits a high degree of symmetry (S_4), which is reflected in a limited set of nonequivalent hydrogen atom

signals in the ^{1}H NMR spectrum. For example, the number of observable nonequivalent hydrogen atoms of R_8BU[4] in the ^{1}H NMR spectrum consists of just three signals, assigned to the *N*-CH_2R groups, methylene groups (NCH_2N) and the methine groups. Unfortunately, Me_8BU[4] has not been prepared; however, the number of limited nonequivalent hydrogen atoms in R_8BU[4] with various alkyl groups (R = Pr, Bn, allyl)[24,25] as well as in *semithio*-Me_8BU[4][20] confirm the high degree of symmetry and the ^{1}H NMR spectra show identical pattern of three signals.

If one of the methyl groups in glycoluril is substituted by a different group (Scheme 2), then a mixture of two enantiomers is obtained. The cyclotetramerization of the glycoluril racemate with paraformaldehyde generates four possible stereoisomers of R_4Me_4BU[4] ($R \neq Me$) (Fig. 1). The ^{1}H NMR spectra of these stereoisomers are expected to differ both in the chemical shift and in the number of nonequivalent protons (number of signals). Indeed, we observed that the ^{1}H NMR spectra of stereoisomers **4a-d** and **5a-d** are remarkably distinct and display variation in the number of nonequivalent hydrogen NMR signal as a result of their singular symmetric environment (*vide infra* Figures 2 & 3). For example, the structure of stereoisomer **5a** exhibits S_4 symmetry. In this arrangement, each of the methyl groups is surrounded by an identical chemical environment, resulting in a single peak at 2.87 ppm (Figure 2, **5a**). Replacement of one of the glycoluril units by its enantiomer (Scheme 2) affords stereoisomer **5b** with C_1 symmetry, which is manifested by the appearance of four different singlets at 2.85, 2.87, 3.06 and 3.07 ppm assigned for each of the four diastereotopic methyl groups (Figure 2, **5b**). Similarly, replacing two neighboring glycoluril units by their enantiomers affords stereoisomer **5c** with S_2 symmetry (inversion) and, consequently, two singlets at 2.85 and 3.08 ppm are observed in the ^{1}H NMR spectrum (Figure 2, **5c**). In contrast, if the two glycouril enantiomers are positioned opposite to each other, then **5d** with C_2 symmetry is obtained, where all four chemically equivalent methyl groups appear at the same chemical shift, in this case at 3.04 ppm (Figure 2, **5d**).

Considering the position of the benzyl group by using the arrowheads drawing presentation (see schematic representation in Figure 1, *bottom*), two types of linking modes between neighboring glycoluril subunits in the 1,3-alternate geometry are defined: “head-to-tail” and “head-to-head” modes. Accordingly, the benzyl groups in **5a** are all arranged in head-to-tail mode and in **5d** the benzyl groups are all arranged in head-to-head mode, whereas stereoisomers **5b** and **5c** exhibit mixed modes. Apparently, these configurations have a profound effect on the chemical shift of the corresponding protons (Figure 2). For example, the neighboring methyl groups in head-to-tail mode undergo a large shielding effect (upfield shift), probably due to an anisotropic effect exerted by the phenyl ring. Thus, the mode by which the substituents are arranged can be unequivocally determined from the chemical shifts in the ^{1}H NMR spectrum.

Further detailed analysis can be inferred from the NMR spectra of **5**, particularly, by identifying all other signals. For instance, the diastereotopic methine protons in **5a** give rise to two-separated AB spin system at 5.59 and 5.52 ppm, each corresponding to 4 protons with a ^3J coupling of 8.4 Hz, which is typical when the vicinal protons are *trans*-coplanar (*i.e.,* the vicinal dihedral angle θ = 0°). In contrast, the chemical shift difference between the coupled methine protons in **5d** is almost indistinguishable. This trend is consistent with other coupled protons of both ^{1}H NMR spectra. Thus, the benzyl protons in **5a** give rise to two doublets at 4.76 and 4.33 ppm, each corresponding to 4 protons with a ^2J coupling of 16 Hz, whereas the observed chemical shift difference between the coupled protons in the ^{1} H NMR spectrum of **5d** is less than 0.1 ppm. Similarly, the bridging methylene protons appear in the spectrum of **5a** at 4.04 and 3.98 ppm as two doublets (^2J = 15.3 Hz), whereas in the spectrum of **5d** these protons

appear as two singlets at 4.64 and 3.76 ppm. These spectroscopic features allow us to identify and discriminate between the linking modes of neighboring glycoluril subunits. Thus, if both benzyl groups are in close proximity to the bridging methylene groups (*e.g.* in **5d**), then the chemical shift differences between the methylene hydrogens will be smaller than the difference when only one of the benzyl groups is in close proximity to the bridging methylene hydrogens (*e.g*. **5a**). Indeed, the two linking modes, head-to-tail and head-to-head, are clearly manifested in the ^{1}H NMR spectra of stereoisomers **5b** and **5c** (marked accordingly in Figure 2).

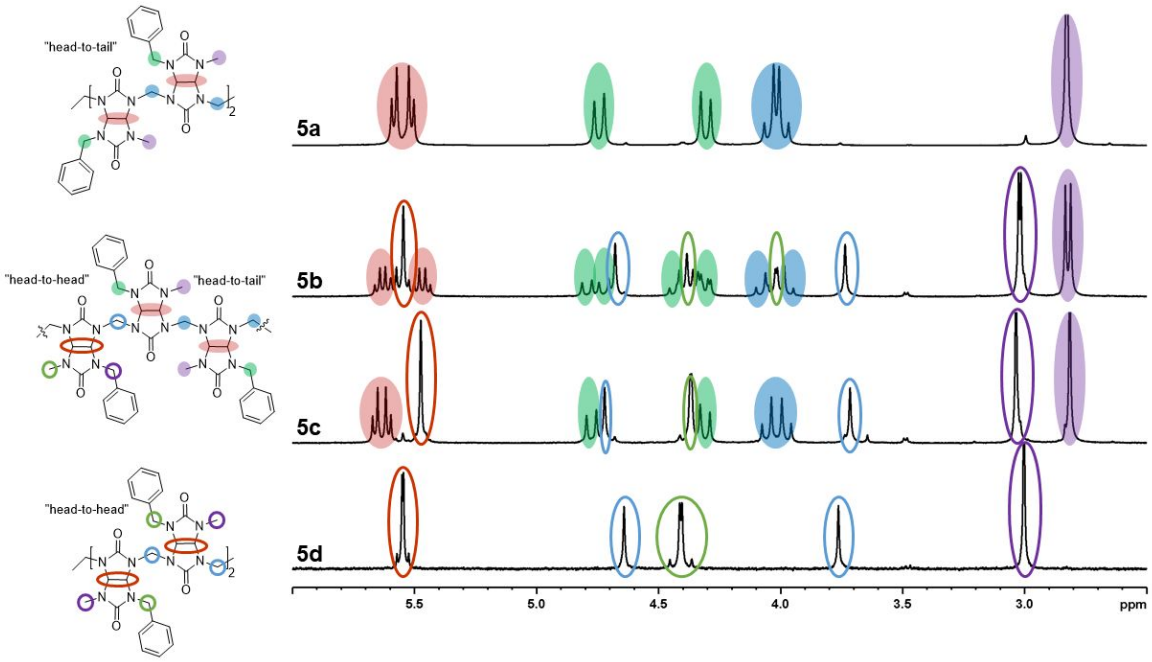

Figure 2. Aliphatic region of the ^{1}H NMR spectra (400 MHz, $CDCl_3$) of stereoisomers of **5**, highlighting the influence of different binding modes on the chemical shift of the corresponding signals.

The chemically nonequivalent methine groups are also evident in the ^{13}C NMR spectrum of **5a** displaying two peaks at 71.9 and 71.6 ppm. Likewise, two separated peaks at 72.1 and 71.2 ppm are observed in the ^{13}C NMR spectrum of **5d**. On the other hand, four signals are observed in the ^{13}C NMR spectra of **5b** and **5c**, confirming the presence of both linking glycoluril modes in the structures of these stereoisomers (see SI Figures S7-S10). 2D-NMR experiments (COSY, HMQC and 2D-NOESY) were recorded and support the structure of each stereoisomer of **5** (Figures S11-S18).

Similar NMR spectroscopy analyses were performed to characterize each stereoisomer of $Pr_4Me_4BU[4]$, **4** (Figure 3 and in SI). Interestingly, the *N*-methyl groups appear as a single singlet at 3.0 ppm corresponding to all 12 methyl protons for all the stereoisomers, except for **4b**. Moreover, replacing all benzyl substituents by propyl groups is obviously manifested by diminished anisotropic effects in the chemical shifts of methine, bridging methylene and *N*-methyl groups. Consequently, the distinction between the linking modes between two neighboring glycoluril subunits in **4** stereoisomers is less evident from their ^{1}H NMR spectra. Nevertheless, the chemical nonequivalence is fully retained for each given type of protons. For example, the chemical shifts of the non-equivalent methine protons are separated by 0.13-0.19 ppm and that of the non-equivalent methylene protons in the propyl groups by 0.35 ppm.

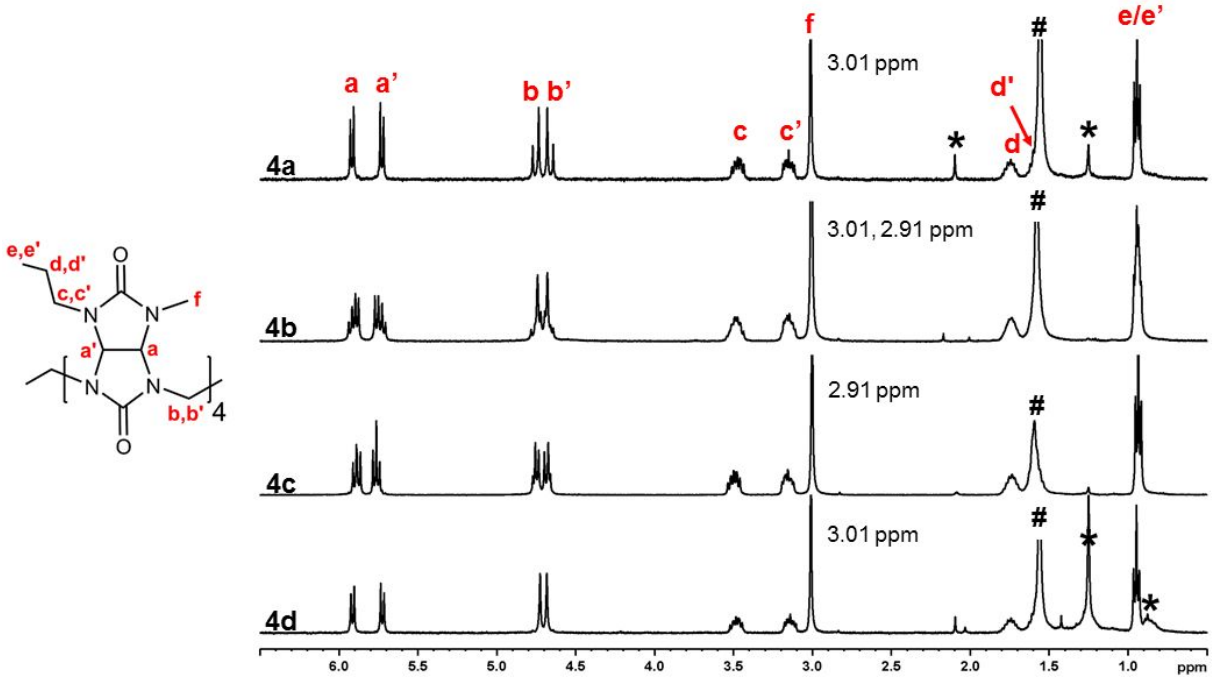

Figure 3. ^{1}H NMR spectra (400 MHz, $CDCl_3$) of stereoisomers of **4**. Hashtag represents the water signal in chloroform and asterisks show solvent impurities.

X-ray crystallography.

The solid-state structures of bambus[4]uril with different substituents was then investigated. Single crystal (Figure 4 and Table 1) of **5a**, suitable for X-ray crystallography, was obtained by slow evaporation of a mixture of $CHCl_3$ and *o*-dichlorobenzene solutions, and the data was collected at 110 K (more crystallographic details in Table S1). Although the phenyl groups are highly disordered and several disordered solvent molecules were observed, we were able to solve the structure by using heavy restrains during refinements (see also Table S1). Expectedly, the rigid structure of **5a** exhibits the 1,3-alternate arrangement of glycoluril subunits, consistent with previously reported solid-state structures of *hetero*-BU[4]s.[24-26] Accordingly, the crystal structure of **5a** is monoclinic, containing four molecules in the unit cell with space group *Cc* and cell constants of a = 23.264(5), b = 18.390(4), c = 17.423(4) Å; and β = 127.66(3)°, respectively. A top view of the crystal structures reveals the relative orientation between substituents (Figure 4A). Hence, in the crystal structure of **5a** all four benzyl groups are oriented anticlockwise in a head-to-tail relationship confirming the anticipated S_4 symmetry.

Recently, four intramolecular distances, d_1-d_4 and a torsional angle, θ (*vide infra*), were defined to characterize the conformations of the various heteroisomers of BU[4].[27] Accordingly, d_1 is the distance between the peripheral carbonyl heteroatoms, d_2 is the distance between the C_2 symmetry related methine carbon atoms, d_3 is the distance between the two equatorial carbonyl oxygen atoms (on the same side), and d_4 is the distance between the planes that include all four methine groups of each portal (Figure 4B). In addition, each glycoluril can be viewed as two rigid flaps fused together at an angle of 113°: one flap participates in the molecular portal whereas the other flap constitutes the molecular equator. Table 1 highlights the similarity of the measured intramolecular distances in **5a** to the values measured in other achiral BU[4] analogues, and that indeed it adopts a double-cup, jigger-like conformation, which is persistently preserved regardless of the nature of their substituents. An analogous trend was also observed for θ, which is defined as the torsion angle between two adjacent flaps that are connected by a

methylene group (see also in Figure 1 colored in red). Hence, in a typical jigger conformation, where $\theta \leq 150^{\circ}$, the portal flaps are effectively perpendicular to one another.

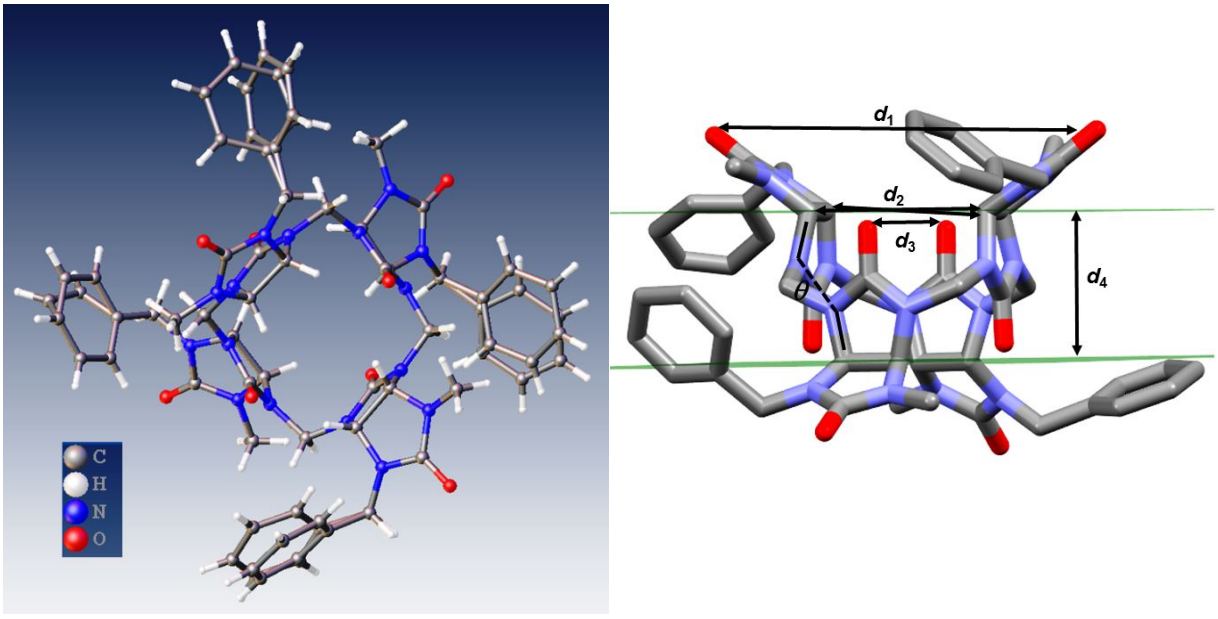

A. **B.**

Figure 4. **A.** Top view of the X-ray single structure of **5a** represented in stick model revealing S_4 symmetry and disordered substituents. Thermal ellipsoids are shown at the 50% probability level. Solvent molecules were omitted for clarity. Color code: nitrogen, blue; oxygen, red; carbon, grey; hydrogen: white. **B.** Side view structure of **5a** as a model used to define distances d_1−d_4 and torsional angle θ.

Table 1. Structural parameters of various BU[4].

Entry	BU[4]	d_1 (Å)	d_2 (Å)	d_3 (Å)	d_4 (Å)	θ (˚)
1	allyl$_8$BU[4][24]	10.6-10.7	5.1-5.5	5.4	3.91	150.6
2	Bn$_8$BU[4][25]	8.5-8.9	4.3-4.9	6.1-6.2	3.93	131.0
3	**5a** (Bn$_4$Me$_4$BU[4])	10.4-10.5	5.0-5.6	5.3-5.5	3.91	148.3

Enantiodifferentiation of chiral bambusurils

Since **4b** and **4d**, as well as **5b** and **5d**, are inherently chiral cavitands, each one of them comprises a pair of enantiomers. Hence, we sought after an efficient technique to resolve them. Initially, attempts were focused on the enantiomeric separation of **5b** by chiral high-performance liquid chromatography (HPLC) techniques. Enantiomer separation of **5b** with various chiral HPLC columns was unsuccessful. In contrast, a satisfactory distinction between enantiomers of **4b** was achieved on a Chiralcel OD-RH® column using water-acetonitrile mixture (65:35, v/v) as eluent (Figure S19). Notably, the separation was better at isocratic conditions. Even though the peak's width increased with retention time, the resulting selectivity factor (α = 1.13) was sufficient to collect each one in high purity (>95 %) by fractional separation.

To circumvent the tedious, expensive and slow chromatographic analytical procedure, and to validate the HPLC separation results, we turned our attention towards alternative enantiodifferentiation methods that could be more straightforward and efficient. Among the commonly used NMR methodologies to investigate enantiomeric separation conditions,[28] we assumed that lanthanide-based chiral shift reagents (LSRs) would be the preferred choice because lanthanides are hard Lewis acids that primarily form complexes with oxygen- and nitrogen-containing donors. However, all attempts to differentiate between the enantiomers of

4b in the presence of Europium(III) tris[3-(hepta-fluoropropylhydroxymethylene)-*d*-camphorate] ($Eu(hfc)_3$) or $Eu(OTf)_3$ failed.

Another commonly used methodology to differentiate between enantiomers comprises chiral solvating agents (CSAs), which form diastereoisomeric solvation complexes with solute enantiomers via rapidly reversible equilibria in competition with the bulk solvent. We investigated a series of chiral 1,1'-bi-2-naphthol (BINOL) derivatives (Figure 5, (*R*)-BINOL **I-V**), which are broadly applicable CSAs, in solutions containing mixtures of all stereoisomers of **4**.

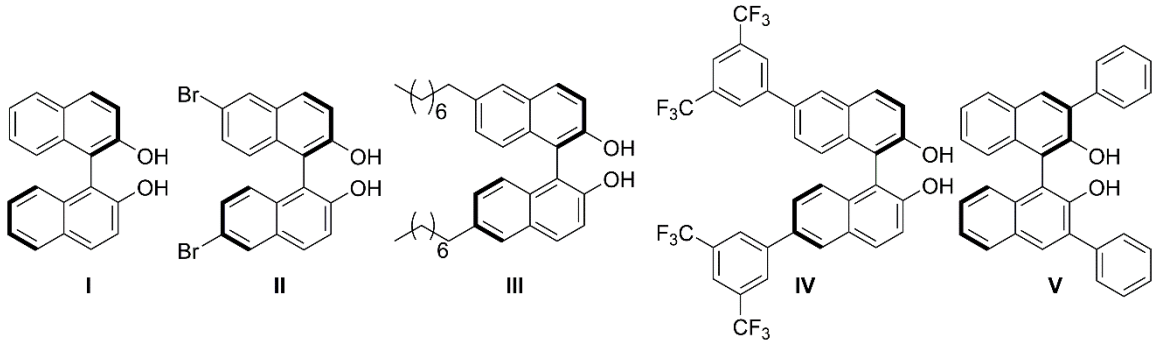

Figure 5. Various chiral BINOL compounds employed as chiral solvating agents in this study.

These atropisomeric compounds can form complexes using the hydroxy groups as hydrogen bond donors and can lead to different chemical shifts for the otherwise undistinguishable enantiomer protons.[29] Indeed, an *in-situ* mixture of all stereoisomers of **4** was treated with BINOL **I** (10 equiv.) giving rise to dramatic changes in the chemical shift values of all ^{1}H NMR signals (Figure 6).

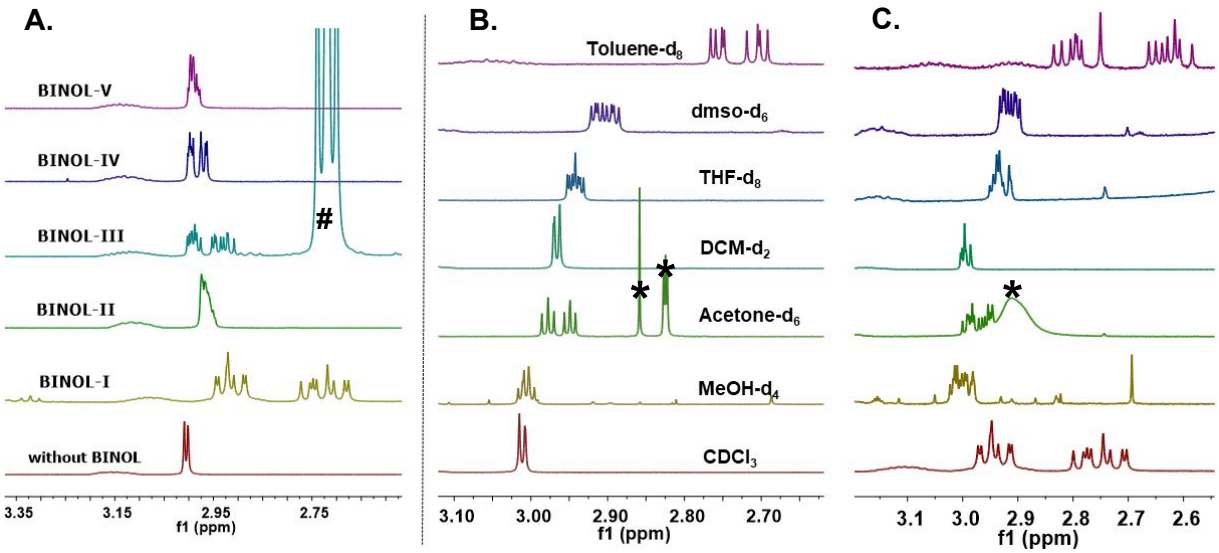

Figure 6. **A**. Fragments of stacked ^{1}H NMR spectra (400 MHz, $CDCl_3$) of a mixture of **4** (3 mg, 1 equiv) diastereoisomers exhibiting δ_H variation of the methyl singlets in the presence of different (*R*)-BINOLs (10 equiv). **B**. ^{1}H NMR spectra (400 MHz) of all **4** (3 mg, 1 equiv) diastereoisomers in different solvents presenting variation in the δ_H of the methyl signals before and **C**. after addition of (*R*)-BINOL **I** (20 equiv). Asterisks refer to residual trace solvent (acetone and water) and hashtag refer to benzylic protons of (*R*)-BINOL **III**.

The analysis of the signals corresponding to the methyl groups of **4** is simpler to monitor because their hydrogen resonances originally appear as two singlets at *ca*. 3.01 ppm and then

split to multiple singlets. To our satisfaction, the recorded spectrum showed almost complete separation of all diastereoisomers, with an average shift of $\Delta\delta_H$ = 0.175 ppm between the stereoisomeric mixture of **4** (δ_{rac} = 3.01 ppm) and their complexes with BINOL **I** ($\delta_{average}$ = 2.825 ppm) (Figure 6A). A similar tendency was observed with (*R*)-BINOLs **II**-**V**, albeit the differences in the chemical shift values for the methyl groups were smaller ($\Delta\delta_H$ = 0.025, 0.060 and 0.013 ppm, respectively) and the signals were less resolved.

Interestingly, a strong solvent effect could also be observed in the NMR mixture. Nonpolar solvents such as chloroform and toluene were shown to maximize the observed anisochrony between the diastereoisomeric complexes after the addition of (*R*)-BINOL **I**, while more polar solvents such as methanol and acetone preferentially solvate BU[4] and the corresponding $\Delta\delta_H$ values were smaller (Figure 6B and 6C). Noticeably, there were no observable changes in the ^{1}H NMR spectrum of **4** in DMSO before and after addition of (*R*)-BINOL **I**. Apparently, DMSO disrupts the BINOL binding to the BU[4].[30].

To elucidate the association between BINOL **I** and stereoisomers of **4**, nuclear Overhauser effect (NOE) spectroscopy was employed. Hence, correlation peaks between several (*R*)-BINOL **I** naphthyl signals and the signals of propyl protons of **4** mixture were clearly detected by 2D ROESY (rotating frame Overhauser spectroscopY),[31] indicating the close proximity of naphthyl rings to the propyl groups (Figure 7).

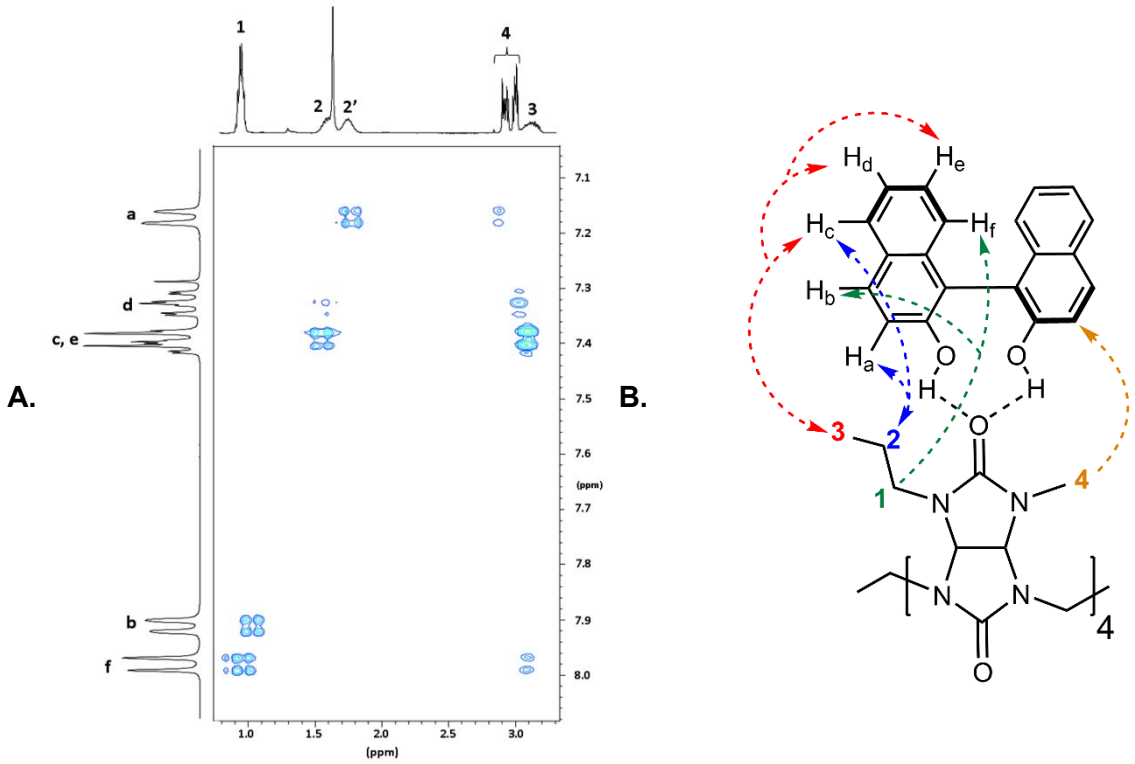

Figure 7: A. Portion of the 2D ROESY spectrum (400 MHz, $CDCl_3$ at 298 K) of (*R*)-BINOL **I** and the mixture of **4** stereoisomers in 5:1 ratio. **B.** Suggested structure of the (*R*)-BINOL **I** complex with $Pr_4Me_4BU[4]$ mixture of all four stereoisomers. Arrows represent the observed intermolecular NOEs between hydrogens of the glycoluril units (H_1, green; H_2, blue; H_3 red; and H_4 yellow) and the corresponding aromatic hydrogens in BINOL molecule (H_{a-f}).

Furthermore, by performing a Job plot analysis the binding stoichiometry of the formed complexes was elucidated[32] (for details see SI). Accordingly, the Job plot displayed a sigmoidal

curvature with a maxima BINOL mol fraction (X_{BINOL}) at 0.5-0.55. This behavior is clearly indicative of 1:1 complex formation.

Following the above results, the applicability of CSA-mediated NMR analysis in enantiodifferentiation between inherently chiral cavitands was probed on the enantiomers of **4b** with (*R*)-BINOL **I**. Recently, CSA-mediated NMR was successfully applied to challenging pharmaceutical development problems, which were not amenable to chromatographic solutions, and provided a rapid and powerful solution for investigating enantiomeric purity that complements and augments conventional chromatographic approaches.[33] Hence, the **4b** enantiomers were separated by chiral HPLC and their ^{1}H NMR spectra were recorded in $CDCl_3$ (Figure 8). Expectedly, both spectra were identical and overlapped the spectrum of the racemic mixture (Figure 8B). However, upon addition of (*R*)-BINOL **I** (5 equiv) the formation of diastereomeric complexes (exhibiting C_1 symmetry) resulted in two sets of four separable singlets assigned for each enantiomer (Figure 8C). The results obtained from the integration of ^{1}H NMR signals for each enantiomer allowed us to estimate the purity of each enantiomer (*ca.* 95 *ee*-%).

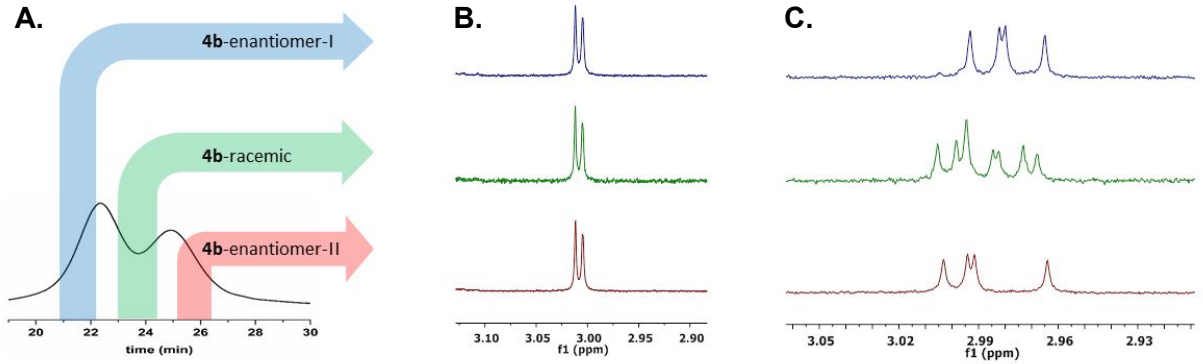

Figure 8: A. HPLC chromatogram displaying separation between enantiomers of *rac*-**4b** on a Chiralcel OD-RH® column (more details in SI); **B**. Fragments of ^{1}H NMR spectra (400 MHz, $CDCl_3$.) of rac-**4b** and its separated enantiomers and **C.** following addition of (*R*)-BINOL **I** (5 equiv).

To validate the generality of this technique in the context of inherently chiral bambusurils, NMR titration of both BINOL **I** enantiomers to a solution containing racemic mixture of **5b** was performed. Upon stepwise addition of (*R*)-BINOL **I** (0.5-20 equiv.), all four-nonequivalent methyl groups in the ^{1}H NMR spectrum of the *racemic* mixture of **5b** displayed an upfield shift and split into eight discrete singlet signals; four singlets for each enantiomer (Figure 9). Interestingly, matching ^{1}H NMR spectra were recorded upon stepwise addition of (*S*)-BINOL **I** (0.5-20 equiv.), indicating that the structures of the formed complexes are symmetrically identical and that both BINOL **I** enantiomers produce identical chemical shift anisochrony. Hence, both enantiomeric BINOL-based solvating agents can be used to discriminate between inherently chiral stereoisomers of BU[4].

In view of the fact that BINOL compounds form weak intermolecular interactions with bambusurils, we also observed changes in the chemical shift pattern of ^{1}H NMR spectra of achiral bambusurils such as **5a** (Figure 10A). Compound **5a** exhibit S_4 symmetry and therefore all four methyl groups display a single singlet signal at δ_H = 2.835 ppm. Upon stepwise addition of *(R)*-BINOL **I** to the solution, the methyl protons peak in **5a** split into two discrete singlets

following complexation with *(R)*-BINOL **l**. Hence, the observed upfield shift of the methyl group signals at $\delta_{complex}$ = 2.82 and 2.765 ppm is explained by the loss of one or more symmetry elements in the structure of **5a**. Consequently, the chemically non-equivalent protons are exposed by their chemical shift differences, which are also concentration-dependent with respect to the added amount of chiral BINOL (as expected for an equilibrium mixture). A similar observation was obtained with *(S)*-BINOL **l** (Figure 10B).

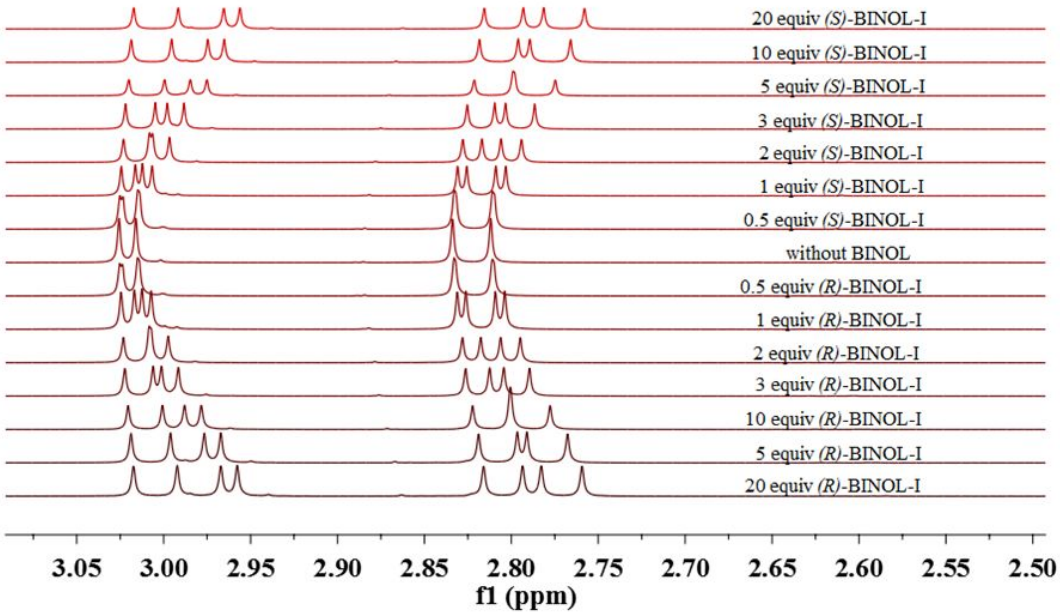

Figure 9. Fragments of stacked spectra from ^{1}H NMR titration (400 MHz, $CDCl_3$) of (*R*)- and *(S)*-BINOL-I with *rac*-**5b** (5 mM).

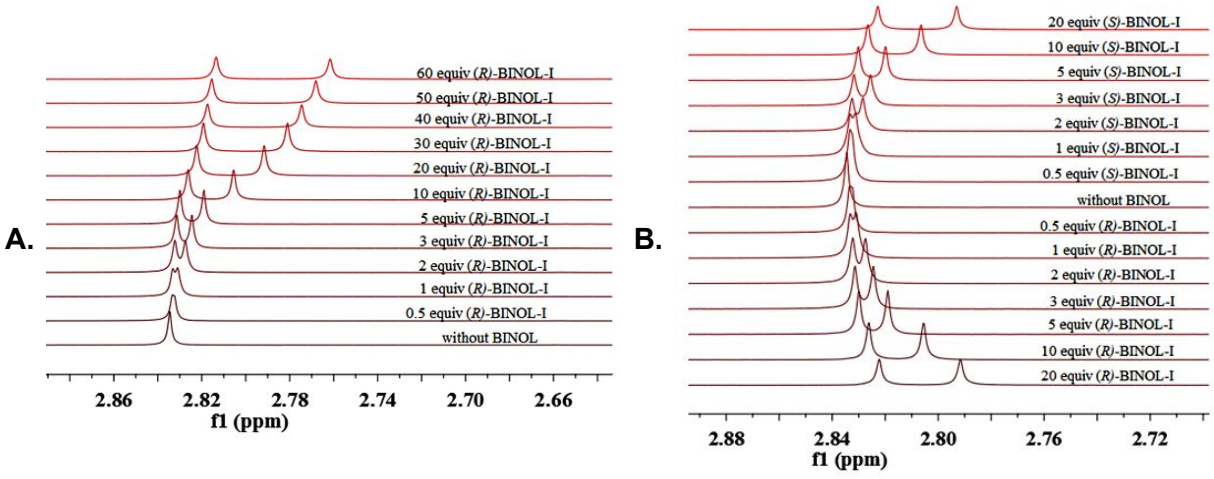

Figure 10. Fragments of stacked spectra from ^{1}H NMR titration (400 MHz, $CDCl_3$) of **5a** (5 mM) with (*R*)-BINOL **l** (0-60 equiv.) (**A**) and with either enantiomer of BINOL **l** (0-20 equiv.) (**B**).

Summary

A series of novel chiral bambus[4]urils containing asymmetric glycoluril subunits with different alkyl substituents have been prepared and all four possible stereoisomers of the $X_4Me_4BU[4]$ family (X = Pr or Bn) have been isolated. These stereoisomers were fully characterized by NMR

techniques and the solid-state structure of **5a**, was analyzed by X-ray crystallography. The crystal structure confirm the induced "head-to-tail" arrangement of the *N*-substituents, following the different spatial orientation of the substituents around the bambusuril cavity. Moreover, it was shown that the different arrangements have a significant effect on the NMR chemical shifts of the corresponding atoms.

All stereoisomers were found to form complexes with chiral BINOLs, probably based on intermolecular hydrogen-bond interactions between the diol moiety of the BINOL molecule and the carbonyl groups at both portals of the bambusuril. These interactions were also evident from the NOE correlations observed between the substituent's protons in the bambusuril molecule and the arene group protons of the BINOL compound.

Finally, the role of BINOL **l** as a chiral solvating agent (CSA) to differentiate between bambusuril stereoisomers was manifested in the ^{1}H NMR spectra of two inherently chiral stereoisomers. The chemical shift differences were found to be markedly dependent on: (1) the nature of solvent, (2) the nature of substituents in the BINOL structure and (3) the extent of CSA necessary for maximal nonequivalence chemical shifts of the enantiopure bambusuril. This methodology provides a rapid and powerful approach for investigating enantiopurity of inherently chiral cavitands, which complements and augments conventional chromatographic approaches.

The new inherently chiral BU[4]s offer interesting opportunities and future applications in the area of supramolecular chemistry. Currently, we are exploring these opportunities with *hetero*-bambusurils in our laboratory.

Experimental Section

General Information. All chemicals, including **1a** and **1b**, and solvents were commercially available and used without further purification. 4,5-dihydroxyimidazolidin-2-one (DHI) was prepared according to ref. 23. Analytical TLC was performed using Merck silica gel F_{254} (230-400 mesh) plates and analyzed by UV light or by staining upon heating with vanilline solution Melting points (mp) were determined in open capillaries using a Stuart SMP11 melting point apparatus. The ^{1}H and ^{13}C NMR spectra were recorded in $CDCl_3$ or DMSO-d_6, on Bruker AVIII400 or Bruker DPX 400 spectrometers. The chemical shifts are reported in parts per million (ppm) relative to residual solvent signals: $CDCl_3$: δ_H = 7.26 ppm, δ_C = 77.23 ppm; DMSO-d_6: δ_H = 2.50 ppm, δ_C = 39.51 ppm.

Single crystals of compound **5a** were obtained by standing a period in *o*-dichlorobenzene-chloroform (1:1) mixture. The single-crystals of each compound were immersed in Paratone–N oil and mounted on an APEX 2 (Bruker AXS) diffractometer at a temperature of 110 K. Data collection was performed with a monochromatic Mo K_a radiation (λ = 0.71073 Å) and using φ and ω scans to cover the Ewald sphere. Using Olex2 program,[34] the structure was solved with the olex2.solve; a structure solution program[35] using Charge Flipping method, and refined with the ShelXL[36] refinement package using Least Squares minimization. Non-hydrogen atoms were refined with anisotropic displacement parameters. The hydrogen atoms were refined isotropically on calculated positions using a riding model with their U_{iso} values constrained to 1.5 times the U_{eq} of their pivot atoms for terminal sp^3 carbon atoms and 1.2 times for all other carbon atoms. Software used for molecular graphics: Mercury 4.0.0.[37]

The chromatographic separation of enantiomers was performed on an YL9100 HPLC System, consisting of a YL9101 Vacuum Degasser, a YL9110 Quaternary Pump and a YL9160 PDA Detector. Chromatographic resolution of enantiomers was carried out on a reverse-phase carbamate-based cellulose (Daicel chemical industries Ltd. Tokyo, Japan) under isocratic and isothermal (at 30 °C) conditions using water/acetonitrile mixture as the appropriate mobile phase giving in the main text. Chiral column was analytical type, dimension 150 mm×4.6mm. Sample preparation: *rac*-**4b** (10 mg) was dissolved in a 65:35 (v/v) mixture of water/acetonitrile (10 mL) with 10 µL of sample solution then injected for HPLC analysis. Detection wavelength: 214 nm.

General procedure for the synthesis of *N,N'*-disubstituted ureas: To a stirred solution of **1a** or **1b** (2 g) in dry THF (10 mL) was added dropwise a solution of methyl amine in THF (2M, 1.5 equiv) at 0 °C. The reaction mixture was stirred at 0 °C for 2 h and then at room temperature for additional 6 h. After removal of the solvent under reduced pressure, the residual precipitate was washed with diethyl ether (DEE, 50 mL) filtered and dried under high vacuum.

1-methyl-3-propylurea (**2a**). White solid (1.9 g, 70% yield). mp 65-67 °C. ^{1}H NMR (400 MHz, $CDCl_3$) δ 5.21 (bs, 2H), 3.11 (q, *J* = 7 Hz, 2H), 2.73 (d, *J* = 4.4 Hz, 3H), 1.47 (sextet, *J* = 7 Hz, 2H), 0.89 (t, *J* = 7 Hz, 3H). ^{13}C{^{1}H} NMR (100 MHz, $CDCl_3$) δ 160.1, 42.5, 27.2, 23.8, 11.7. HRMS (ESI) m/z: $[M - H]^-$ Calcd for $C_9H_{11}N_2O$ 163.0871; Found 163.0870.

1-benzyl-3-methylurea (**2b**). White solid (2.12 g, 86% yield). mp 95-96 °C. ^{1}H NMR (400 MHz, DMSO-d_6) δ 7.32–7.19 (m, 5H), 6.37 (bt, *J* = 5.6 Hz, 1H), 5.81 (bq, *J* = 4.4 Hz, 1H), 4.21 (d, *J* = 6.4 Hz, 2H), 2.58 (d, *J* = 4.4 Hz, 3H); ^{13}C{^{1}H} NMR (100 MHz, DMSO-d_6) δ 159.6, 142.0, 129.1, 127.9, 127.4, 43.9, 27.4; HRMS (ESI) m/z: $[M - H]^-$ Calcd for $C_9H_{11}N_2O$ 163.0871; Found 163.0870.

General procedure for the synthesis of *N,N'*-disubstituted glycolurils: A suspension solution containing 4,5-dihydroxyimidazolidin-2-one (1 g, 8.5 mmol) and urea **2a** or **2b** (1 equiv) in water (3 mL) were heated up to 60 °C under vigorous stirring and conc. HCl (35%, 0.15 mL) was added. Then the heating temperature was raised and kept at 105 °C for additional 75 min. Upon cooling, the gummy precipitate solidified and then filtered, washed with water and dried under high vacuum to afford **3a** or **3b** respectively.

1-methyl-3-propyl-tetrahydroimidazo-[4,5-d]imidazole-2,5(1H,3H)-dione (**3a**). White solid (1.2 g, 71% yield). m.p. 265-266 °C; ^{1}H NMR (400 MHz, DMSO-d_6) δ 7.52 (s, 1H), 7.49 (s, 1H), 5.23 (dd, *J* = 8 Hz and 1 Hz, 1H), 5.13 (dd, *J* = 8 Hz and 1 Hz, 1H), 3.16–3.09 (m, 1H), 2.97–2.91 (m, 1H), 2.63 (s, 3H), 1.58–1.37 (m, 2H), 0.82 (t, *J* = 7.4 Hz, 3H); ^{13}C{^{1}H} NMR (100 MHz, DMSO-d_6) δ 162, 158.6, 68.3, 66.5, 43.5, 28.6, 21.5, 12.1; HRMS (ESI) m/z: $[M - H]^-$ Calcd for $C_8H_{13}N_4O_2$ 197.1039; Found 197.1037.

1-benzyl-3-methyl-tetrahydroimidazo[4,5-d]imidazole-2,5(1H,3H)-dione (**3b**). White solid (1.55 g, 75% yield). mp 215-216 °C; ^{1}H NMR (400 MHz, DMSO-d_6) δ 7.61 (s, 1H), 7.58 (s, 1H), 7.35–7.32 (m, 2H), 7.28–7.24 (m, 3H), 5.16 (dd, *J* = 8 Hz and 1.6 Hz, 1H), 5.03 (dd, *J* = 8 Hz and 1.6 Hz, 1H), 4.60 (d, *J* = 15.6 Hz, 1H), 4.01 (d, *J* = 15.6 Hz, 1H), 2.69 (s, 3H); ^{13}C{^{1}H} NMR (100 MHz, DMSO-d_6) δ 162, 158.4, 138.4, 129.4, 128.7, 128.1, 68.2, 65.9, 44.8, 28.7; HRMS (ESI) m/z: $[M - H]^-$ Calcd for $C_{12}H_{13}N_4O_2$ 245.1039; Found 245.1030.

General procedure for the synthesis of BU[4] derivatives.[38] A mixture containing compound **3a** or **3b** (0.246 g, 0.1 mol), paraformaldehyde (36 mg, 1.2 equiv) and *p*-toluene sulfonic acid (0.172g, 1 equiv) in $CHCl_3$ (10 mL) was subjected to microwave irradiation for 2 h

under continuous stirring at 75 °C (P_{max} = 200 watt, *T* = 75 °C). Then the reaction mixture was cooled and diluted with $CHCl_3$ (30 mL). The organic layer was washed with saturated $NaHCO_3$ (50 mL), water (50 mL) and brine (50 mL), and the organic layer was dried over anhydrous Na_2SO_3. After filtration, the solution was concentrated. After addition of diethyl ether, the bambusuril stereoisomer mixture was precipitated as white solid immediately thereafter. After filtration and washing with diethyl ether, the white solid was dried under high vacuum. The mixture of stereoisomer products was re-dissolved in $CHCl_3$ and run on preparative thin layer chromatography (PTLC) with ethyl acetate as mobile phase to give each of the diastereoiasomers of either **4a-d** or **5a-d** isolated in the following ratio: **4a**:**4b**:**4c**:**4d** (1:1:1:1) or **5a**:**5b**:**5c**:**5d** (0.8:1:1:0.6).

$Pr_4Me_4BU[4]$ (**4**, as mixture of diastereoisomers): White solid (0.173 g, 69% yield). ^{1}H NMR (400 MHz, $CDCl_3$) δ 5.93–5.85 (m, 16H), 5.77–5.69 (m, 16H), 4.77-4.63 (m, 32H), 3.53-3.42 (m, 16H), 3.18-3.10 (m, 16H), 3.00 (s, 24H), 2.99 (s, 24H), 1.74-1.71 (m, 16H), 1.62-1.52 (m, 16H), 0.95-0.91 (m, 48H); ^{13}C{^{1}H} NMR (100 MHz, $CDCl_3$) δ 159.9, 159.8, 158.2, 158.2, 72.5, 72.4, 70.6, 70.52, 70.46, 70.38, 52.1, 51.96, 51.83, 51.69, 51.54, 51.42, 51.29, 44.57, 30.20, 30.15, 30.10, 30.05, 30.02, 21.45, 21.39, 11.60, 11.55.

$Pr_4Me_4BU[4]$ (**4a**). White solid; ^{1}H NMR (400 MHz, $CDCl_3$) δ 5.93 (d, *J* = 8 Hz, 4H), 5.74 (d, *J* = 8 Hz, 4H), 4.61 (dd, *J* = 16 Hz and 20 Hz, 8H), 3.51–3.44 (m, 4H), 3.19–3.11 (m, 4H), 3 (s, 12H), 1.80 (sextet, *J* = 8 Hz, 4H), 1.62 (sextet, *J* = 8 Hz, 4H), 0.96 (t, *J* = 8 Hz, 12H); ^{13}C{^{1}H} NMR (100 MHz, $CDCl_3$) δ 159.8, 158.2, 72.4, 70.6, 51.3, 44.6, 30.2, 30, 21.5, 11.6.

$Pr_4Me_4BU[4]$ (**4b**). White solid; ^{1}H NMR (400 MHz, $CDCl_3$) δ 5.92 (dd, *J* = 8 Hz, 4H), 5.77 (dd, *J* = 8 Hz, 4H), 4.78–4.64 (m, 8H), 3.54–3.44 (m, 4H), 3.18–3.11 (m, 4H), 3.01 (s, 6H), 3 (s, 6H), 1.74 (bs, 4H), 1.62 (bs, 4H), 0.96 (sextet, *J* = 4 Hz, 12H); ^{13}C{^{1}H} NMR (100 MHz, $CDCl_3$) δ 159.8, 158.2, 72.7, 72.6, 72.5, 72.4, 70.6, 70.5, 70.49, 70.4, 69.8, 52, 51.9, 51.6, 51.5, 44.6, 30.2, 30.1, 21.5, 21.4, 21.3, 11.6, 11.58; HRMS (ESI) m/z: $[M + H]^+$ Calcd for $C_{36}H_{57}N_{16}O_8$ 841.4545; Found 841.4555.

$Pr_4Me_4BU[4]$ (**4c**). White solid; ^{1}H NMR (400 MHz, $CDCl_3$) δ 5.91 (t, *J* = 8 Hz, 4H), 5.78 (t, *J* = 8 Hz, 4H), 4.77–4.66 (m, 8H), 3.54–3.46 (m, 4H), 3.19–3.12 (m, 4H), 3 (s, 12H), 1.80 (sextet, *J* = 8 Hz, 4H), 1.64 (sextet, *J* = 8 Hz, 4H), 0.97 (t, *J* = 8 Hz, 12H); ^{13}C{^{1}H} NMR (100 MHz, $CDCl_3$) δ 160, 159.8, 158.2, 158.19, 72.6, 72.4, 70.5, 70.4, 51.8, 51.7, 51.6, 44.7, 44.6, 30.1, 30, 21.4, 11.6; HRMS (ESI) m/z: $[M + H]^+$ Calcd for $C_{36}H_{57}N_{16}O_8$ 841.4545; Found 841.4555.

$Pr_4Me_4BU[4]$ (**4d**). White solid; ^{1}H NMR (400 MHz, $CDCl_3$) δ 5.92 (d, *J* = 8 Hz, 4H), 5.74 (d, *J* = 8 Hz, 4H), 4.73 (d, *J* = 20 Hz, 8H), 3.52–3.45 (m, 4H), 3.18–3.10 (m, 4H), 3.01 (s, 12H), 1.80 (sextet, *J* = 8 Hz, 4H), 1.64 (sextet, *J* = 8 Hz, 4H), 0.97 (t, *J* = 8 Hz, 12H); ^{13}C{^{1}H} NMR (100 MHz, $CDCl_3$) δ 159.8, 158.2, 72.5, 70.5, 51.8, 44.6, 30.2, 21.5, 11.6.

$Bn_4Me_4BU[4]$ (**5**, as mixture of diastereoisomers): White solid (0.158 g, 63% yield).

$Bn_4Me_4BU[4]$ (**5a**). White solid; ^{1}H NMR (400 MHz, $CDCl_3$) δ 7.34–7.24 (m, 20H), 5.59 (d, *J* = 8.4 Hz, 4H), 5.52 (d, *J* = 8.4 Hz, 4H), 4.76 (d, *J* = 16.0 Hz, 4H), 4.33 (d, *J* = 16.0 Hz, 4H), 4.04 (d, *J* = 16 Hz, 4H), 3.98 (d, *J* = 16 Hz, 4H), 2.83 (s, 12H); ^{13}C{^{1}H} NMR (100 MHz, $CDCl_3$) δ 159.3, 158.6, 137.7, 129.2, 128, 127.9, 72.3, 71.9, 51, 47.8, 29.9; HRMS (ESI) m/z: $[M + H]^+$ Calcd for $C_{52}H_{57}N_{16}O_8$ 1033.4545; Found 1033.4539.

$Bn_4Me_4BU[4]$ (**5b**). White solid; ^{1}H NMR (400 MHz, $CDCl_3$) δ 7.35–7.23 (m, 16H), 7.16–7.13 (m, 4H), 5.66–5.44 (m, 8H), 4.81–4.64 (m, 4H), 4.46–4.29 (m, 6H), 4.10–3.95 (m, 4H), 3.75 (s, 2H), 3.03 (s, 3H), 3.015 (s, 3H), 2.83 (s, 3H), 2.81 (s, 3H); ^{13}C{^{1}H} NMR (100 MHz, $CDCl_3$) δ

159.62, 159.34, 159.29, 158.97, 158.64, 158.59, 158.52, 158.44, 137.67, 137.62, 137.27, 137.18, 129.19, 129.18, 129.12, 128.11, 128.08, 128.06, 128.03, 127.88, 127.86, 127.83, 72.46, 72.42, 72.16, 71.78, 71.55, 71.27, 51.33, 51.23, 51.19, 50.84, 47.81, 47.76, 47.25, 30.29, 30.26, 29.95, 29.81; HRMS (ESI) m/z: $[M + H]^+$ Calcd for $C_{52}H_{57}N_{16}O_8$ 1033.4545; Found 1033.4540.

$Bn_4Me_4BU[4]$ (**5c**). White solid; ^1H NMR (400 MHz, $CDCl_3$) δ 7.33–7.27 (m, 16H), 7.15–7.14 (m, 4H), 5.67 (d, 8.4 Hz, 2H), 5.62 (d, 8.4 Hz, 2H) 5.47 (s, 4H), 4.80 (d, *J* = 16 Hz, 2H), 4.72 (s, 2H), 4.37 (d, *J* = 2 Hz, 4H), 4.33 (d, *J* = 16 Hz, 2H), 4.08 (dd, *J* = 20 Hz and 16 Hz, 4H), 3.72 (s, 2H), 3.04 (s, 6H), 2.82 (s, 6H); $^{13}C\{^1H\}$ NMR (100 MHz, $CDCl_3$) δ 159.6, 159, 158.6, 158.5, 137.6, 137.3, 129.2, 129.1, 128.1, 128, 127.9, 127.9, 72.6, 72.3, 72, 71.3, 51.6, 51, 47.7, 47.3, 30.2, 29.9; HRMS (ESI) m/z: $[M + H]^+$ Calcd for $C_{52}H_{57}N_{16}O_8$ 1033.4545; Found 1033.4540.

$Bn_4Me_4BU[4]$ (**5d**). White solid; ^1H NMR (400 MHz, $CDCl_3$) δ 7.30-7.28 (m, 12H), 7.17 (m, 8H), 5.57 (dd, *J* = 8.4 Hz and 2.4 Hz, 8H), 4.64 (s, 4H), 4.45 (dd, *J* = 16 Hz and 4 Hz, 8H), 3.76 (s, 4H), 3.00 (s, 12H);$^{13}C\{^1H\}$ NMR (100 MHz, $CDCl_3$) δ 159.4, 158.5, 137.2, 129.1, 128.1, 127.8, 72.4, 71.6, 51.2, 47.2, 30.3; HRMS (ESI) m/z: $[M + H]^+$ Calcd for $C_{52}H_{57}N_{16}O_8$ 1033.4545; Found 1033.4578.

ASSOCIATED CONTENT

Supporting Information

The Supporting Information is available free of charge on the ACS Publication website at DOI: 101021/acs.joc.XXXXXX. Details of the X-ray structural characterization and NMR studies of both characterization, and CSA titrations:
SI file (PDF)
X-ray data for **5a** (CIF)

AUTHOR INFORMATION

Corresponding Author

∗E-mail: oferre@openu.ac.il

ORCID
Amar Mohite: 0000-0001-6039-7028
Ofer Reany: 0000-0003-1048-1947

ACKNOWLEDGMENTS

Financial support for this work was provided by The Ministry of Science Technology and Space (MOST grant No. 3-10855). We thank Dr. Natalia Fridman from the crystallographic lab at the Schulich Faculty of Chemistry, Technion, for her valuable contribution to the X-ray crystallographic efforts. We thank Prof. Doron Pappo from Department of Chemistry, Ben-Gurion University of the Negev for providing optically pure *(R)*-BINOL II-V derivatives for this study. We also thank Prof. N. Gabriel Lemcoff for his valuable comments on this manuscript.

REFERENCES

1. Scriba, G. K. E. in *Chiral separations: methods and protocols*, 3rd Ed., Humana Press, 2019.
2. Evans, N. H.; Beer, P. D. Chirality in the host-guest behavior of supramolecular systems. In *Chirality in supramolecular assemblies: causes and consequences*; Keene, F. R. (Ed) Wiley, 2017, chapter *5*, 142-158.
3. (a) Fankhauser, D.; Easton, C. J. Chirality in organic hosts. In *Chirality in supramolecular assemblies: causes and consequences*; Keene, F. R. (Ed) Wiley, 2017, chapter 11, 307-342; (b) Breslow, R.; Dong S. D. Biomimetic reactions catalyzed by cyclodextrins and their derivatives. *Chem. Rev.* **1998**, *98*, 1997-2011.
4. Chao, Y.; Weisman, G. R.; Sogah, G. D. Y.; Cram, D. J. Host-guest complexation. 21. Catalysis and chiral recognition through designed complexation of transition-states in transacylations of amino ester salts. *J. Am. Chem. Soc.* **1979**, *101*, 4948-4958.
5. (a) Collman, J. P.; Fu, L. Synthetic models for hemoglobin and myoglobin. *Acc. Chem. Res.*, **1999**, *32*, 455–463; (b) Feiters, M. C.; Rowan, A. E.; Nolte, R. J. M. From simple to supramolecular cytochrome P450 mimics. *Chem. Soc. Rev.* **2000**, *29*, 375-384.
6. (a) Gokel, G. W.; Leevy, W. M.; Weber, M. E. Crown ethers: sensors for ions and molecular scaffolds for materials and biological models. *Chem. Rev.* **2004**, *104*, 2723-2750; (b). Gokel, G. W.; Carasel, I. A. Biologically active, synthetic ion transporters. *Chem. Soc. Rev.* **2007**, *36*, 378-389.
7. (a) Aav, R.; Shmatova, E.; Reile, I.; Borissova, M.; Topić, F.; Rissanen, K. New chiral cyclohexyl hemi-cucurbit[6]uril. *Org. Lett.*, **2013**, *15*, 3786-3789; (b) Prigorchenko, E.; Öeren, M.; Kaabel, S.; Fomitšenko, M.; Reile, I.; Järving, I.; Tamm, T.; Topi´c, F.; Rissanen, K.; Aav. R. Template-controlled synthesis of chiral cyclohexylhemicucurbit[8]uril. *Chem. Commun.* **2015**, *51*, 10921–10924; (c) Kaabel, S.; Adamson, J.; Topić, F.; Kiesilä, A.; Kalenius, E.; Öeren, M.; Reimund, M.; Prigorchenko, E.; Lõokene, A.; Reich, H. J.; Rissanen, K.; Aav, R. Chiral hemi-cucurbit[8]uril as an anion receptor: selectivity to size, shape and charge distribution. *Chem. Sci.*, **2017**, *8*, 2184-2190; (d) Lisbjerg, M.; Pittelkow, M. Hemi-cucurbit[*n*]urils. In *Comprehensive Supramolecular Chemistry II*; Atwood, J. L., (*Ed.*) Elsevier, Oxford, 2017, vol. 3, pp. 221–236; (e) Kaabel, S.; Aav, R. Templating effects in the dynamic chemistry of cucurbiturils and hemicucurbiturils. *Isr. J. Chem.*, **2018**, *58*, 296–313; (f) Andersen, N. N.; Lisbjerg, M.; Eriksen, K.; Pittelkow, M. Hemicucurbit[n]urils and their derivatives – synthesis and applications. *Isr. J. Chem.*, **2018**, *58*, 435–448.
8. (a) Lisbjerg, M.; Jessen, B. M.; Rasmussen, B.; Nielsen, B. E.; Madsen, A. Ø.; Pittelkow, M. Discovery of a cyclic 6 + 6 hexamer of D-biotin and formaldehyde. *Chem. Sci.*, **2014**, *5*, 2647-2650; (b) Lisbjerg, M.; Nielsen, B. E.; Milhøj, B. O.; Sauer, S. P. A.; Pittelkow, M. Anion binding by biotin[6]uril in water. *Org. Biomol. Chem.*, **2015**, *13*, 369-373.
9. Sokolov, J.; Sindelar V. Chiral bambusurils for enantioselective recognition of carboxylate anion guests. *Chem.-Eur. J.* **2018**, *24*, 15482 – 15485.
10. Mclldowie, M. J.; Mocerino, M.; Ogden, M. I. A brief review of C_n-symmetric calixarenes and resorcinarenes. *Supramol. Chem.* **2010**, *22*.13-39.
11. Bohmer, V.; Kraft. D.; Tabatabai, M. Inherently chiral calixarenes. *J. Inclu. Phenom. Mol. Recog. Chem.* **1994**, *19*, 17-39.
12. Cort, A. D.; Mandolini, L.; Pasquini, C.; Schiaffino, L. “Inherent chirality” and curvature. *New. J. Chem.*, **2004**, *28*, 1198-1199.
13. Szumna, A. Inherently chiral concave molecules – from synthesis to applications. *Chem. Soc. Rev.*, **2010**, *39*, 4274-4285.
14. Arnott, G. E. Inherently chiral calixarenes: synthesis and applications. *Chem.-Eur. J.* **2018**, *24*, 1744-1754.
15. Mandadapu, V.; Day, A. I.; Ghanem, A. Cucurbituril: chiral applications. *Chirality*, **2014**, *26*, 712-723.
16. Huang, W.-H.; Zavalij, P. Y.; Isaacs, L. Chiral recognition inside a chiral cucurbituril. *Angew. Chem. Int. Ed.*, **2007**, *46*, 7425-7427.
17. Huang, W.-H.; Liu, S.; Zavalij, P. Y.; Isaacs L. *nor-seco*-Cucurbit[10]uril exhibits homotropic allosterism. *J. Am Chem. Soc.* **2006**, *128*, 14744-14745.

18. Cheng, X.-J.; Liang, L.-L; Chen, K.; Ji, N.-N.; Xiao, X.; Zhang, J.-X.; Zhang, Y.-Q.; Xue, S.-F.; Zhu, Q.-J.; Ni, X.-L.; Tao, Z. Twisted cucurbit[14]uril. *Angew. Chem. Int. Ed.* **2013**, *52*, 7252 –7255 .
19. For recent review see: Reany, O.; Mohite, A.; Keinan, E.; hetero-Bambusurils. *Isr. J. Chem.* **2018**, *58*, 449 –460.
20. Singh, M.; Solel, E.; Keinan, E.; Reany, O. Dual-functional semithio-bambusurils. *Chem. Eur. J.* **2015**, *21*, 536-540.
21. Mondal, P.; Solel, E.; Fridman, N.; Keinan, E.; Reany, O. Intramolecular van der Waals interactions challenge anion binding in *perthio*-Bambusurils. *Chem. Eur. J.* **2019**, *25*, 13336 – 13343.
22. Kunturu, P. P.; Kap O.; Sotthewes, K.; Cazade, P.; Zandvlient, H. J. W.; Thompson, D.; Reany, O.; Huskens, J. Anchoring and packing of self-assembled monolayers of semithio-bambusurils on Au(111). *Mol. Sys. Des. Eng.* **2020**, *5*, 511-520.
23. Correia, H. D.; Cicolani, R. S.; Moral, R. F.; Demets, G. J. F. Easy synthesis of trans-4,5-dihydroxy-2-imidazolidinone and 2,4-dimethylglycoluril. *Synth.* **2016**, *48*, 210-212.
24. Rivollier, J.; Thuery, P.; Heck, M.-P. Extension of the bambus[n]uril family: microwave synthesis and reactivity of allylbambus[n]uril. *Org. Lett*. **2013**, *15*, 480-483.
25. Havel, V.; Svec, J.; Wimmerova, M.; Dusek, M.; Pojarova, M.; Sindelar, V. Bambus[n]urils: a new family of macrocyclic anion receptors. *Org. Lett.* **2011**, *13*, 4000-4003.
26. Singh, M.; Solel, E.; Keinan, E.; Reany, O. Aza-Bambusurils *E*n-route to anion transporters. *Chem. Eur. J.* **2016**, *22*, 8848-8854.
27. Mondal, P.; Solel, E.; Shubhanjan, M.; Keinan, E.; Reany, O. Equatorial Sulfur Atoms in Bambusurils Spawn Cavity Collapse. *Org. Lett.*, **2020**, *22*, 204-208.
28. Parker, D. NMR determination of enantiomeric purity. *Chem. Rev.* **1991**, *91*, 1441-1457.
29. Wenzel, T. J.; Chisholm, C. D. Using NMR spectroscopic methods to determine enantiomeric purity and assign absolute stereochemistry *Prog. Nucl. Magn. Reson. Spectrosc.* **2011**, *59*, 1-63.
30. Ni, X.; Li, X.; Li, Z.; Cheng, J.-P. Equilibrium acidities of BINOL type chiral phenolic hydrogen bonding donors in DMSO. *Org. Chem. Front.* **2016**, *3*, 1154-1158.
31. Neuhaus, D.; Williamson, M. P. in *The nuclear Overhauser effect in structural and conformational analysis*. 2nd ed., WILEY-VCH, New York, **2000**.
32. Gil, V. M. S.; Olivereira, N. C. On the use of the method of continuous variations. *J. Chem. Educ.* **1990**, *67*, 473-478.
33. Yang, L.; Wenzel, T.; Williamson, R. T.; Christensen, M.; Schafer, W.; Welch, C. J. Expedited selection of NMR chiral solvating agents for determination of enantiopurity. *ACS Cent. Sci*. **2016**, *2*, 332−340.
34. Dolomanov, O. V.; Bourhis, L. J.; Gildea, R. J; Howard, J. A. K.; Puschmann, H. OLEX2: a complete structure solution, refinement and analysis program. *J. Appl. Cryst.* **2009**, *42*, 339-341.
35. Bourhis, L. J.; Dolomanov, O. V.; Gildea, R. J.; Howard, J. A. K.; Puschmann, H. The anatomy of a comprehensive constrained, restrained refinement program for the modern computing environment - Olex2 dissected. *Acta Cryst*. **2015**, *A71*, 59-75.
36. Sheldrick, G.M. SHELXT - Crystal structure refinement with SHELXL. *Acta Cryst*. **2015**, *C71*, 3-8.
37. Mercury Software from CCDC: http://www.ccdc.cam.ac.uk/Solutions/CSDSystem/Pages/Mercury. aspx.
38. The synthetic procedure described here can be also performed under heating in oil bath at the same temperature but longer reaction time is required (24 h).